Development of an optoelectronic nose based on surface plasmon resonance imaging with peptide and hairpin DNA for sensing volatile organic compounds

Sara Gaggiotti[a], Charlotte Hurot[b], Jonathan S. Weerakkody[b], Raphael Mathey[b], Arnaud Buhot[b], Marcello Mascini[a], Yanxia Hou[b,*], Dario Compagnone[a,*]

[a] Università degli Studi di Teramo, Via Renato Balzarini, 1, 64100, Teramo, Italy
[b] Univ. Grenoble Alpes, CEA, CNRS, IRIG, SyMMES, F-38000, Grenoble, France

ABSTRACT

Nowadays, the analysis of volatile organic compounds (VOCs) is very important in various domains. In the last decades, electronic noses have emerged as promising alternatives to traditional analytical methods. Nevertheless, their wide use is still limited by their performances such as low selectivity. Herein, we developed an optoelectronic nose using virtually screened peptides and hairpin DNA (hpDNA) with improved selectivity as sensing materials and surface plasmon resonance imaging (SPRi) as the detection system. Thanks to the complementarity of their binding properties towards target VOCs, the obtained optoelectronic nose has very good selectivity, being able to discriminate not only between VOCs of different chemical families, but also VOCs of the same family with only 1-carbon difference. The combination of these sensing materials with SPRi is relevant for the development of optoelectronic nose with large sensor arrays and improved performances.

1. Introduction

Monitoring volatile organic compounds (VOCs) is crucial in many domains including air quality control, diagnosis of certain diseases through the detection of volatile markers in breath, quality control for food and in the cosmetic industry. Gas chromatography and mass spectroscopy are very powerful and reliable systems with high accuracy in the analyses of VOCs, but are known to be expensive, time-consuming, demanding in the pretreatment of samples and requiring trained operators. Electronic noses (eNs), in the form of gas sensor arrays, are promising alternatives that proved to be particularly useful for the rapid and on-site detection of VOCs [1].

One of the major challenges with such systems is the design and development of novel sensing materials for improved performances, thereby, the improvement in sensitivity and selectivity [2]. By mimicking the biological olfactory system, some researchers have employed biomaterials such as olfactory receptors, odorant binding proteins (OBPs), and synthetic olfactory receptor-based polypeptides [3–5] for VOC sensing. The obtained olfactory biosensors can be highly sensitive and selective. Nevertheless, the integration of such biomolecules into eNs is often limited by their stability.

In such a context, peptides are particularly promising as sensing

materials for the detection of VOCs thanks to their homology to biomolecules and their chemical robustness. Moreover, today, they can be easily synthesized. Finally, they can be further modeled and virtually screened in order to obtain better selectivity and specificity to VOCs of interest. Indeed, virtual screening methodology allows 'in silico' testing of VOC - peptide binding in a fast and low-cost way. Moreover, it offers considerable assistance for the understanding of molecular interaction, and for the identification of candidate compounds as new ligands. In some recent studies, molecular modeling has been successfully used to rationally design synthetic receptors for a variety of analytical applications, both in liquid [6–9] and in gas [10]. In our previous work, we have demonstrated that peptides selected by virtual screening are very efficient materials for sensing VOCs in food samples such as olive oil [11], chocolate [12], candies [13], fruit juices [14], carrots [15], and pasta [16].

Another molecular family with great potential as sensing materials for the detection of VOCs is DNA. The use of DNA in the field of analytical applications has attracted great interest in last decades, mostly using DNA sensors for the analysis of liquid samples [17,18]. More recently, gas sensors have been successfully developed with DNA as sensing materials [19–21]. In our previous study, for the first time, we have designed and selected several hairpin DNA (hpDNA) for gas

sensing. The shape of these sequences was very interesting because it maximized the orientation of the binding element (via the stem) using the loop as a sensitive element. In addition, the binding affinity between hpDNA loop and different VOCs was investigated based on in-silico calculation [22].

In previous works peptide-based gas sensors and hpDNA-based gas sensors were separately assembled using quartz crystal microbalances (QCMs) with six sensors in parallel. These sensing materials were first immobilized onto gold nanoparticles, used as a platform in order to increase the sensitivity of the system, and then deposited onto QCM crystals. However, multiplexing to obtain a large sensor array is limited in this configuration. For this, herein, both peptides and hpDNA will be used as sensing materials on the same chip for the development of an optoelectronic nose employing surface plasmon resonance imaging (SPRi) as transduction system. SPRi has been largely used for the development of biochips for monitoring biomolecular binding events [19–21] as well as the development of electronic tongues for the analysis of proteins [23] and complex mixtures in liquid [24–26]. Recently, we have demonstrated its efficiency for the development of olfactory biosensors using OBPs [27]. Furthermore, in another study, for the first time, we have proven that SPRi is very efficient for the development of the eNs for sensing VOCs in gas phase [28]. Eighteen sensing molecules including cross-reactive short peptides and thiols, with diverse physicochemical properties were self-assembled directly on the gold surface of the prism and used for gas sensing showing very high sensitivity and selectivity. The obtained eN has several advantages over other existing eNs, capable of simultaneously monitoring all binding events on a large sensor array (> 300 sensors) in real time, label-free, and with temporal responses containing important kinetic information. To further improve the performances of the optoelectronic nose such as sensitivity and selectivity, it is important to integrate more selective sensing materials and to increase their diversity. Therefore, in this study, we intend to develop and evaluate the performance of a novel optoelectronic nose by coupling the SPRi transduction techniques with these new sensing materials for the analysis of VOCs. Moreover, SPRi will allow us to directly compare the performances of peptides and hpDNA on the same chip without the use of nanoparticles for the signal amplification, in contrast with QCM. Our final objective is to develop a larger sensor array combining their binding properties to improve the performances of the optoelectronic nose.

2. Material and methods

2.1. Reagents and chemicals

Different chemical classes of volatile organic compounds were analyzed. 1-butanol ($\geq$ 99.4%), 1-pentanol ($\geq$ 99%), 1-hexanal ($\geq$ 95%), 1-nonanal ($\geq$ 95%), trans-2-nonenal ($\geq$ 95%) and 1-hexanoic acid ($\geq$ 98%) were purchased from Sigma-Aldrich. Six sequences of penta-peptide (TGKFC, KSDSC, IHRIC, WHVSC, LAWHC, LGFDC), containing a terminal cysteine for their immobilization on the prism, were purchased from Espikem (Italy, purity > 85%). In the supplementary section, Fig. S1 shows the functional groups within the peptide structures. Three sequences of hpDNA with unpaired tetramer loops (CGGG, GTTG, CCAG) were purchased from Thermo Fischer Scientifics (Italy); while, pentamer (TAAGT, AAGTA, CCCGA) and hexamer (CATGTC, ATAATC, CTGCAA) loops were purchased from Integrated DNA Technologies (USA).

The nine ssDNA loops (CGGG, GTTG, CCAG, TAAGT, AAGTA, CCCGA, CATGTC, ATAATC and CTGCAA) were then extended and synthesized with the same double helix stem of four base pair DNA (GAAG to 5′ end and CTTC to 3′ end). The purified oligonucleotides also had a thiol spacer having six carbons (C6) attached to 5′ phosphate end of the hpDNA.

Each HpDNA secondary structure was analyzed using the Mfold Web Server (www.unafold.rna.albany.edu) to check the stem-loop intramolecular base pairing. Fig. S2, in supplementary material, shows the most thermodynamically favorable structures of hpDNA at 25 °C, obtained by the Mfold Web Server. This temperature was the one kept in experimental testing. At this temperature, all selected DNA should have the desired structure.

2.2. Preparation of the chip

All peptides and hpDNA were immobilized onto a prism covered with a thin gold layer to form a microarray (Fig. S3). 48 h prior to use, the prism was treated by plasma (generated at 0.6 mbar with 75% Oxygen and 25% Argon, at a power of 40 W for 3 min) using the Femto plasma cleaner (Diener Electronic, Germany). Then, drops of 1.2 nL of peptide and hpDNA aqueous solution containing 5% glycerol were deposited in a microarray format using a non-contact micro-spotting instrument (Scienion AG, Germany). The chip was put in a small chamber at 25 °C with a controlled humidity and was left overnight. As a result, peptides and hpDNA were immobilized on the chip by self-assembly. At the beginning of the study, different concentrations of peptides and hpDNA were used for the optimization of their density on the chip. Moreover, each solution was spotted in quadruplicates on the prism in a random position. Before the first use, the chip was rinsed to wash away the unfixed receptors, dried under a flow of argon, and stored at 4 °C.

2.3. SPR imaging set-up and VOC analysis

The detection of VOCs was evaluated with a home-made SPRi system and its set-up was described in a previous work [28]. This instrument, designed for gas sensing, is based on the Kretschmann configuration where a collimated polarized beam at 632 nm is sent towards the gold surface to illuminate the whole microarray. When the VOCs interact with the receptors on the chip, an alteration in local refractive index occurs, resulting in a shift of the resonance angle of the surface plasmon. Herein, the gas sensing analysis was done at a fixed working angle, chosen to maximize the sensitivity and minimize noise. In such a way, the interaction between VOCs and receptors will generate a variation of the reflectivity, which is monitored and recorded with a 16-bit CCD video camera. Thanks to this imaging mode, we can follow simultaneously the interaction of a VOC sample with all receptors on the chip. According to the differential affinity, the spots of the receptors light up at different gray levels.

The VOC sample headspace is processed and conveyed to the analysis cell in the SPRi apparatus by a fluidic circuit, which contains a sample line and a reference line of only dry air. Before VOC analysis, a blank injection of dry air was performed for two minutes to ensure the cleanliness of the analyte line. In conjunction, the baseline was checked to ensure a very minimal drift. To perform the VOC analysis, 50 μL of pure liquid VOC were introduced in a glass bottle to generate a dynamic headspace. The evaporated VOC was transported to the analysis cell through the sample line for 10 min with a constant flow rate (dry air at 100 mL min^{-1}) and pressure (50 mbar above ambient). These parameters were controlled using mass-flow and pressure controllers (Bronkhorst, Netherlands). Moreover, the analysis cell is connected to a photoionization detector (PID) (ppbRAE300, RAE Systems, U.S.) for the measurement of VOC concentration at the outlet. After each injection, the system was regenerated and rinsed with dry air for 10–20 min, by switching to the reference line. The whole SPRi apparatus was put in a Peltier controlled incubator set at 25 °C in order to avoid temperature effects.

2.4. Data treatment

The dataset obtained in real time was the mean raw reflectivity (% R) of the spot of interest. It was then converted into a variation of reflectivity Δ%R. Moreover, for the statistics study, Δ%R was normalized

(Rnorm) in order to avoid the VOC concentration effect. The normalization was run according to Hines, E. L et al. [29] Eq. (1), where N was the number of receptors.

$$\text{Rnorm (CRRn)} = \frac{\Delta\%R_{CRRn}}{\sqrt{\Sigma_{n=1}^{N} \Delta\%R_{CRRn}^2}} \cdot \sqrt{N} \tag{1}$$

Finally, Principal Component Analysis (PCA) and Agglomerative Hierarchical Clustering (AHC) analysis using XLSTAT software (Addinsoft, New York, NY) were performed to better understand and explain the dataset.

3. Results and discussion

For this study, six penta-peptides and nine hpDNA, previously selected using a virtual screening method, were used [10,21]. The virtual binding properties of the peptides and hpDNA were calculated against different VOCs belonging to different chemical classes (e.g. alcohols, aldehydes, etc.). H-bonds and conformation were found to be the key elements for the binding. Using peptides, 5 units plus a linker (cysteine) was selected as the minimum length to have good affinity while hpDNA affinity improved with unpaired loop size. For linkers having the same structure the association complexes having H-bonds are expected to give higher binding scores.

3.1. Optimization on the chip preparation

We have initially optimized spotting volumes and receptor concentrations in order to prepare chips with homogeneous spots and good receptor densities. The spotting volume is an important parameter; by decreasing it, more receptors and replicates can be put on the chip to obtain a large sensor array. However, if the volume is too small, there is a risk of drop evaporation during self-assembly of peptides and hpDNA during overnight incubation, thus resulting in non-reproducible and non-homogeneous spots. Herein, six penta-peptides and nine hpDNA in quadruplicate were deposited on the chip. To avoid evaporation, 5% glycerol was added in peptide and hpDNA aqueous spotting solutions. After spotting, the chip was put in a small chamber, overnight, with controlled temperature and humidity. Three spotting volumes (1.2 nL, 2.0 nL, 4.0 nL) were tested. Satisfyingly, there were no observable drop size reduction for any of them. Most importantly, all obtained spots on the chip were homogeneous, even 1.2 nL. Therefore, this was chosen as the spotting volume in this study. Different concentrations of peptides (100 μM, 200 μM, 400 μM, 800 μM) and hpDNA (3.4 μM, 6.7 μM, 16.8 μM) in the spotting solutions were then tested in order to optimize receptor density on the chip. Fig. 1 shows the gray scale values of the spots obtained with the penta-peptides and hpDNA at different concentrations for comparison. The gray scale value reflects the density of

molecules that were immobilized on the chip. The values obtained with peptides and hpDNA were comparable. For penta-peptides, increasing the concentration from 100 μM to 200 μM led to significant increase for gray scale value. Nevertheless, in most of the cases, a plateau was reached at 200 μM. It seems that at higher concentrations the density of peptide molecules reached its maximum. Therefore, this concentration was chosen for the chip preparation. As for hpDNA, lower concentrations were used taking into account of the loop structure and the cost (3.4 μM, 6.7 μM, 16.8 μM). In such a concentration range, for most of the cases, the higher the hpDNA concentration, the higher their density on the chip. As a compromise between good receptor density and amount of molecules used, 16.8 μM of hpDNA was used for the rest of the study.

3.2. Analysis of various VOCs with optoelectronic nose

In this study, five different target VOCs (1-butanol, 1-pentanol, 1-hexanal, 1-nonanal, trans-2-nonenal) were selected from two different chemical families (alcohol and aldehyde) in order to evaluate their affinity with peptides and hpDNA.

Fig. 2a and b show two examples of sensor responses obtained with 1-butanol and 1-nonanal, with a sample injection for 10 min followed by rinsing with dry air. First and foremost, it was noticed that all penta-peptides and hpDNA were very sensitive to these VOCs, producing good signals, without using nanoparticles for signal amplification. Each sequence of penta-peptides and hpDNA gave different responses to a given VOC. Moreover, the kinetic sensor responses of the two VOCs were very different from each other. To better illustrate the discrimination capacity of the optoelectronic nose, for each analyzed VOC, its characteristic differential SPRi image and response pattern were given, as shown in Fig. 2c–g. The response pattern in the form of histograms represents the variation of reflectivity for all penta-peptides and hpDNA at equilibrium (10 min after the beginning of the sample injection), where the average value and the standard deviation between the different quadruplicates are given. It is evident that their SPRi images and thereby their response patterns are distinct. Therefore, they can be used as quick response (QR) code, a unique respective barcode, for VOC identification.

3.3. Pearson correlation: peptides and hpDNA

In order to have a picture of the relations between the peptides and the hpDNA responses, the Pearson correlation coefficients were computed and reported in Table. 1. Correlation coefficients vary between −1 and 1. Negative values indicate negative correlation, and positive values indicate positive correlations. Values close to zero reflect the absence of correlation.
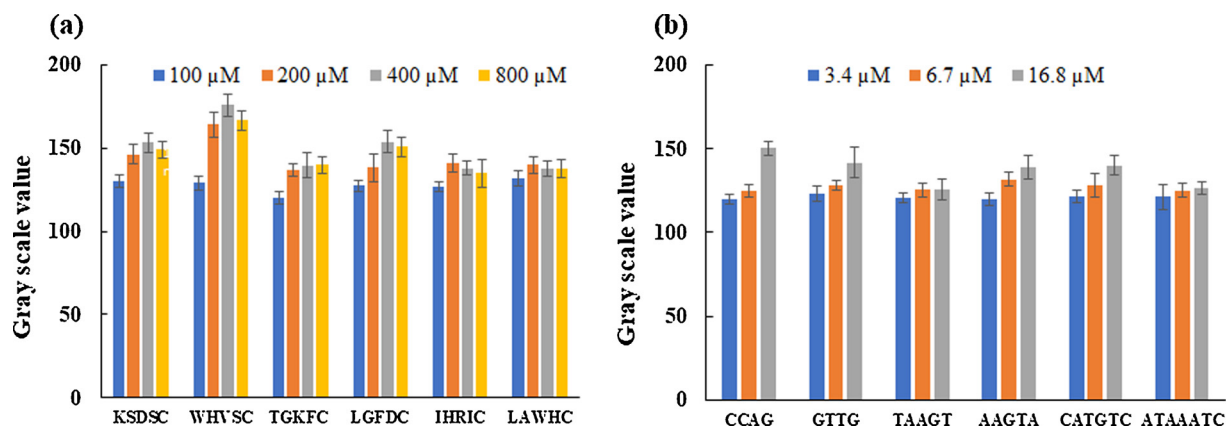

Fig. 1. Gray scale value of the spots corresponding to a) the six penta-peptides at different concentrations (100 μM, 200 μM, 400 μM, 800 μM) and b) six hpDNA at different concentrations (3.4 μM, 6.7 μM, 16.8 μM).
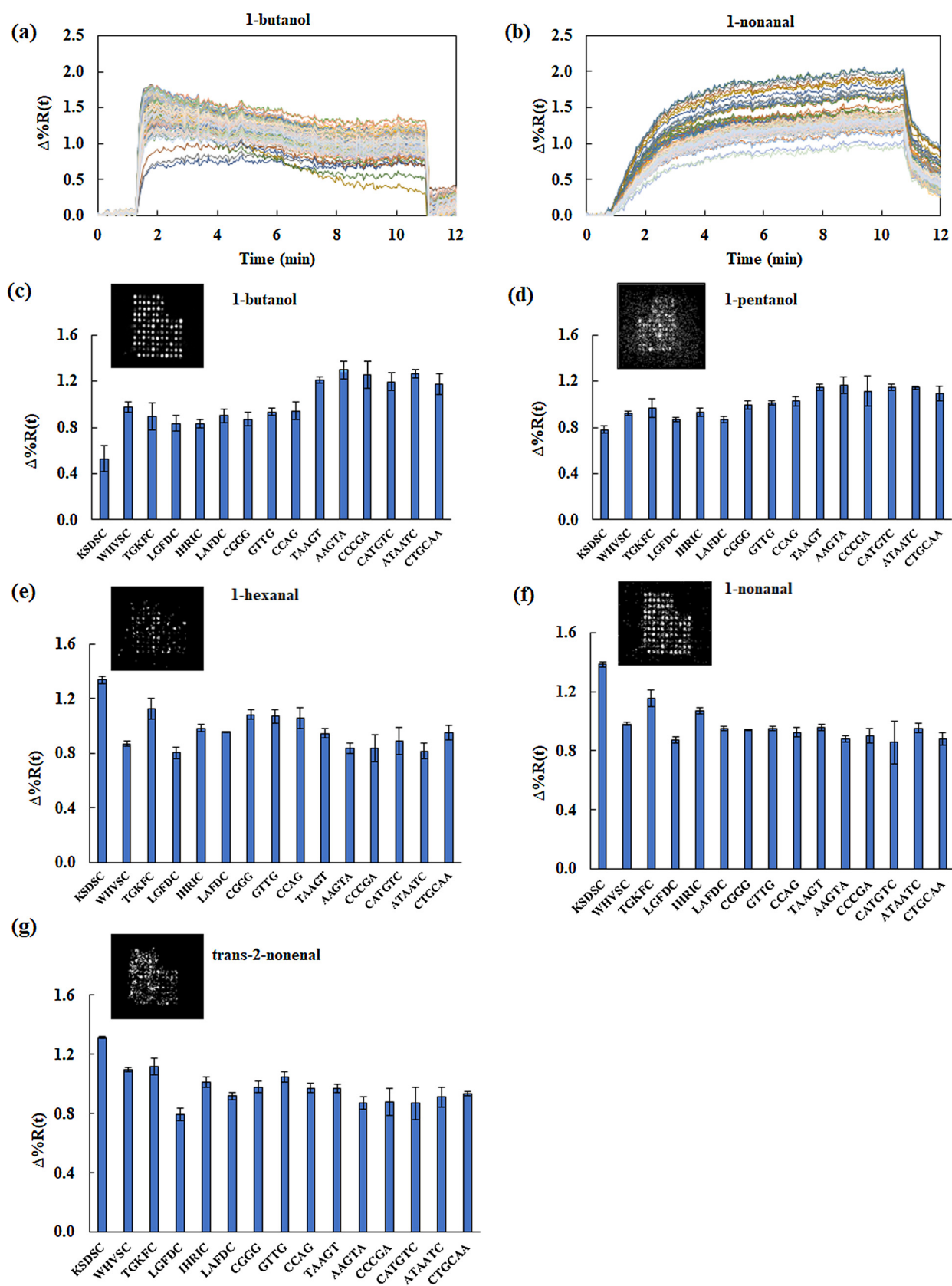
Fig. 2. Example of sensor responses after exposure to a) 1-butanol and b) 1-nonanal. Response patterns and characteristic SPRi images at equilibrium for c) 1-butanol (55 ppm), d) 1-pentanol (31 ppm), e) 1-hexanal (90 ppm), f) 1-nonanal (3.6 ppm) and g) trans-2-nonenal (7.0 ppm).

Table 1
Correlation coefficients between peptides and hpDNA.

	KSDSC	WHVSC	TGKFC	LGFDC	IHRIC	LAWHC			
KSDSC	1.00								
WHVSC	0.00	1.00							
TGKFC	0.71	0.15	1.00						
LGFDC	−0.21	0.50	0.19	1.00					
IHRIC	0.72	−0.34	0.44	−0.50	1.00				
LAWHC	0.19	0.61	0.42	0.56	−0.32	1.00			
	KSDSC	WHVSC	TGKFC	LGFDC	IHRIC	LAWHC			
CGGG	0.39	−0.71	−0.11	−0.80	0.64	−0.64			
GTTG	0.28	−0.64	0.00	−0.84	0.63	−0.69			
CCAG	0.10	−0.77	0.01	−0.70	0.56	−0.72			
TAAGT	−0.92	0.19	−0.53	0.49	−0.82	−0.01			
AAGTA	−0.87	0.30	−0.63	0.43	−0.86	0.19			
CCCGA	−0.68	0.51	−0.38	0.58	−0.83	0.52			
CATGTC	−0.86	0.04	−0.49	0.48	−0.70	−0.13			
ATAATC	−0.73	0.50	−0.42	0.70	−0.88	0.33			
CTGCAA	−0.85	0.09	−0.59	0.29	−0.88	0.00			
	CGGG	GTTG	CCAG	TAAGT	AAGTA	CCCGA	CATGTC	ATAATC	CTGCAA
CGGG	1.00								
GTTG	0.82	1.00							
CCAG	0.71	0.85	1.00						
TAAGT	−0.62	−0.45	−0.32	1.00					
AAGTA	−0.60	−0.62	−0.50	0.86	1.00				
CCCGA	−0.77	−0.78	−0.69	0.74	0.92	1.00			
CATGTC	−0.46	−0.35	−0.20	0.93	0.72	0.56	1.00		
ATAATC	−0.81	−0.79	−0.70	0.87	0.91	0.91	0.73	1.00	
CTGCAA	−0.45	−0.40	−0.28	0.87	0.87	0.73	0.75	0.77	1.00

The correlations among peptides showed higher variability than among hpDNA. For peptides, there are two groups, one including KSDSC, TGKFC, and IHRIC, and a second one including WHVSC, LGFDC, and LAWHC. There is a more positive correlation between the peptides of the same group. On the other hand, hpDNA with tetramer loops correlated positively with each other while negatively correlating to pentamer and hexamer loops. A strong positive correlation was observed between the hpDNA pentamer and hexamer loops. Comparing peptides and hpDNA, hpDNA with tetramer loops negatively correlated with WHVSC, LGFDC, LAWHC and slightly positively correlated with KSDSC, IHRIC but not with TGKFC. HpDNA pentamer and hexamer loops were partially positively correlated to the peptides WHVSC, LGFDC, LAWHC but very negatively correlated with the other three peptides KSDSC, TGKFC and IHRIC. Therefore, these data further confirmed that peptides and hpDNA may give differential responses for the tested VOCs.

3.4. Multivariate data analysis

The contributions of peptides and hpDNA for the discrimination between the analyzed VOCs were then explored using multivariate analysis. The signal obtained for the 1-hexanoic acid, injected to eliminate the possible interferences between different injection of compounds [27], was also included in the dataset as a negative control. The dataset obtained by SPRi was treated by principal component analysis (PCA) to better highlight the contribution of each sensing material for the discrimination of VOCs. First, peptides and hpDNA were analyzed as two separated datasets and reported in Figs. 3 and 4.

Fig. 3 shows the scores and loading plots of the first two principal components that correspond to 79.45% of the total variance of the data. The PC1 shows clear discrimination between 1-hexanoic acid and the other VOCs. The PC2 contributes mainly to the separation of aldehydes (1-hexanal, 1-nonanal, trans-2-nonenal) from the other VOCs in the upper half of the PCA. The three different chemical classes were well discriminated. Moreover, a good separation was obtained for 1-butanol and 1-pentanol. However, based on these results it is hard to discriminate among the three aldehydes.

Penta-peptides have differential binding affinity for VOCs of different chemical classes, which was dependent on the structure and reactivity of VOCs. Thus, they have selectivity in binding according to chemical classes. The virtual binding affinity data showed that penta-peptides TGKFC, KSDSC and IHRIC had better interactions with VOCs with longer chain, preferentially having a carbonyl group, whereas other penta-peptides WHVSC, LAWHC, LGFDC had a good affinity towards short chain VOCs. [10,14]. Indeed, as shown in Fig. 3b, the peptides LAWHC, WHVSC and LGFDC had similar responses showing higher affinity for small chain alcohol such as 1-butanol. While the peptides TGKFC, KSDSC and IHRIC had higher interaction with longer chain molecules such as 1-nonanal.

Fig. 4 shows the response of hpDNA with the first two principal components representing 89.26% of the total variance of the data. Here again, good separation was obtained for the three chemical classes but not for the three aldehydes. The in-silico screening for hpDNA [22] showed that the presence of more bases in the loop can contribute synergistically in binding VOCs. The tetramer loops showed a good affinity towards small aldehydes while the pentamer and hexamer loops demonstrated stronger interaction with alcohols. This is consistent with our observation. The hpDNA with pentamer and hexamer loops along PC1 highlighted a higher binding affinity to 1-butanol and 1-pentanol, while tetramer loops had more affinity for 1-hexanal.

In order to have a more reliable classification by including more dimensionality of the data in the statistical analysis, the two datasets were analyzed by an unsupervised hierarchical clustering method. This allowed increasing the data-to-variable ratio and a more reliable classification was obtained (Fig. 5). To enhance discrimination among molecules the agglomerated hierarchical clustering (AHC) algorithm was applied. AHC begins with each individual object (e.g. sample) in a single cluster. Then, in each subsequent iteration, it agglomerates (unites) the closest cluster pair by satisfying some similarity criteria, until all the data are in a cluster. The results obtained by this type of clustering state that the greater the distance between the samples the better the discrimination [30].

Fig. 5 reports the dendrogram based on the steady state signal of the data set obtained with penta-peptides or hpDNA loops. Using the penta-
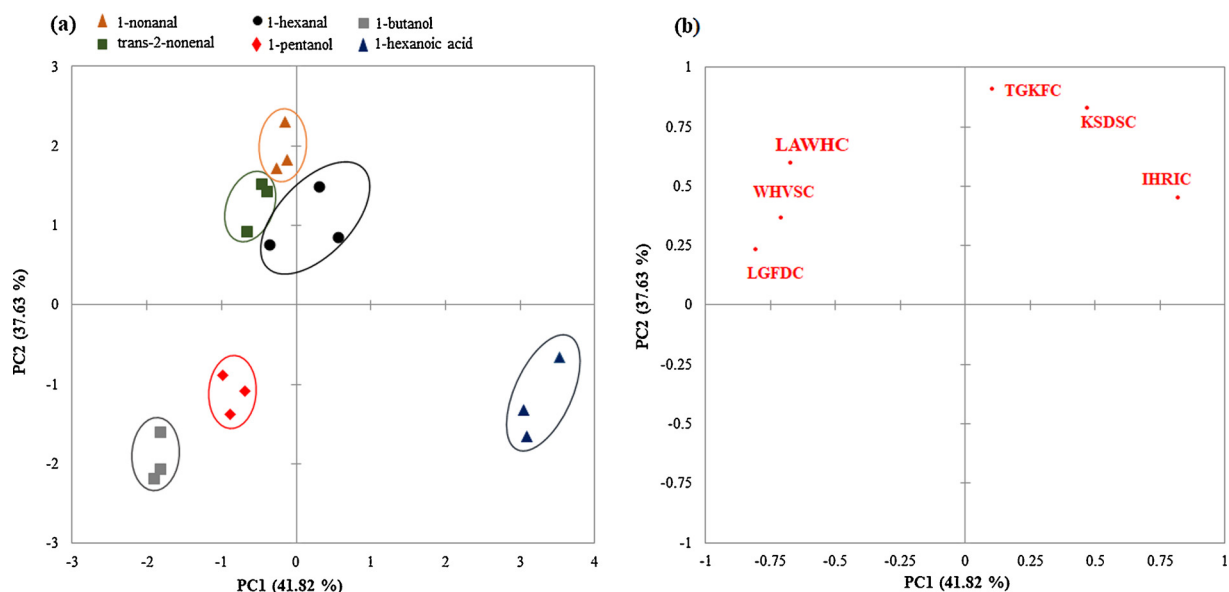
Fig. 3. PCA (*score* and *loading* plots) for the discrimination of different VOCs with different penta-peptides. On the left, the score plot reporting analyzed VOCs. On the right, the loadings plot reporting the contribution of the penta-peptides.

peptides (Fig. 5a), the different chemical classes analyzed were separated very well without overlap (1-pentanol and 1-butanol - green line / 1-hexanoic acid purple line / trans-2-nonenal, 1-nonanal, and 1-hexanal - orange line). Similar results were obtained with hpDNA (Fig. 5b). However, using hpDNA, it is difficult to discriminate among the three aldehydes (purple line) since trans-2-nonenal overlaps both with nonanal and hexanal; on the other hand all alcohols (green line) and 1-hexanoic acid (orange line) were separated very well. These results demonstrated that the optoelectronic nose consisting of either short peptides or hpDNA with different loop size, allowed to discriminate between different chemical classes. The better performance of peptides in classification could be justified by the higher diversity of their physicochemical properties thanks to greater combinations of diverse amino acids as basic brick when compared to DNA, composed of only four bases. In the latter case the selectivity was related to the size of the loop and not to a particular combination of the bases.

Finally, we have evaluated the performances of the optoelectronic

nose by combining the responses of peptides and hpDNAs using PCA plots and AHC dendrograms (Fig. 6). The PCA (Fig. 6a) shows a good separation for all chemical classes analyzed with the first two principal components representing 83.09% of the total variance of the data. AHC dendrograms (Fig. 6b) shows the same results obtained with PCA, in fact, looking at the different color lines is possible to observe that there is a perfect separation between the chemical classes: 1-butanol and 1-pentanol (green line), trans-2-nonenal, 1-nonanal, and 1-hexanal (purple line), and 1-hexanoic acid (orange line). Clearly, the performance of the optoelectronic nose was improved because of the greater distance among classes. The better discrimination ability for tested being related to the complementarity of the response. All the data reported demonstrate that the optoelectronic nose has very good selectivity, being able to discriminate not only between VOCs of different chemical families, but also VOCs of the same family with even only 1-carbon difference such as 1-butanol and 1-pentanol.
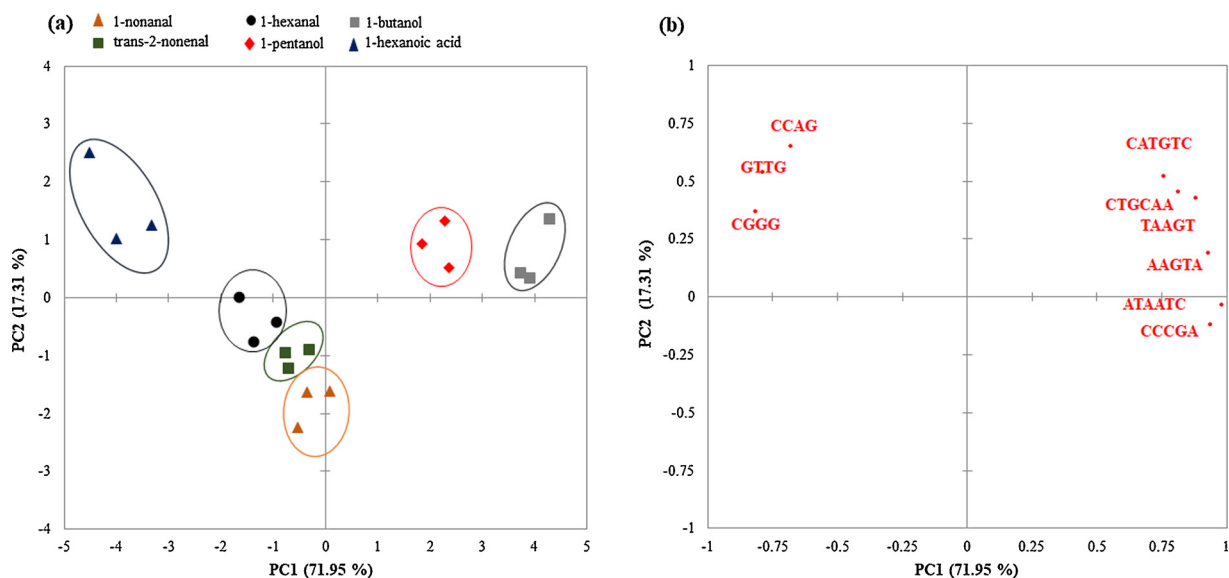

Fig. 4. PCA (*score* and *loading* plots) for the discrimination of different VOCs with different hpDNA. In the left the score plot reporting VOCs analyzed. In the right the loadings plot reporting the contribution of the hpDNA with different loops (4; 5 and 6) reported in red.
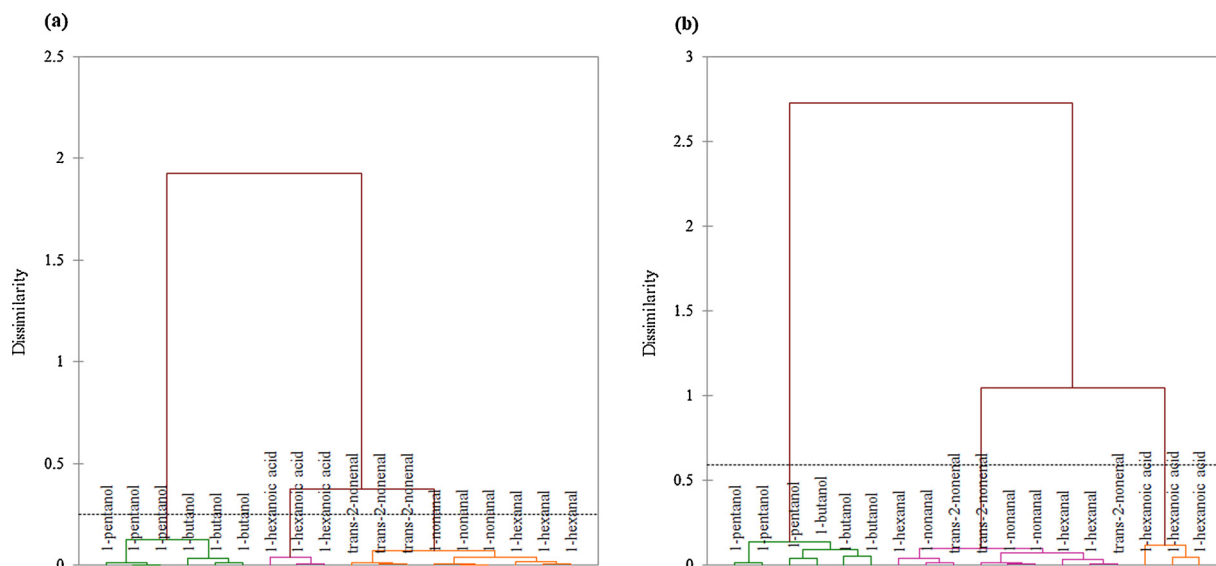
(a)

(b)

Fig. 5. AHC results obtained with peptides and hpDNA for the analysis of different VOCs.
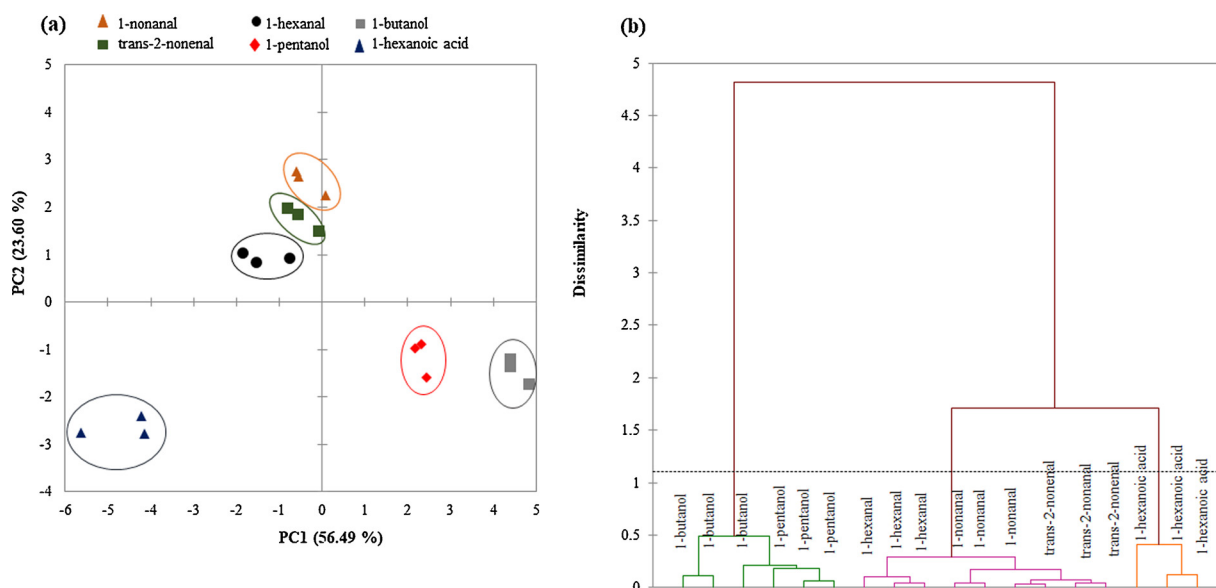
(a)

(b)

Fig. 6. a) PCA plots and b) AHC dendrograms for the discrimination of different VOCs by combining the responses of peptides with those of hpDNA.

4. Conclusion

In this work, we developed an optoelectronic nose using virtually screened peptides and hpDNA with improved selectivity as sensing materials and SPRi as the detection system. It is able to discriminate not only between VOCs of different chemical families, but also VOCs of the same family with only 1-carbon difference, thanks to the complementarity on the binding properties of peptides and hpDNA for target VOCs. By combining these sensing materials with SPRi, it is relevant for the development of optoelectronic nose with large sensor arrays and improved performances so as to narrow the performance gap between electronic noses and human nose. In the future, we will design other novel peptides and hpDNA specific for some VOCs with high societal impact and integrate them into portable devices for the rapid and on-site analysis. Such devices can be useful in various domains such as indoor and outdoor air quality monitoring, detection of olfactory pollution, food quality control, food safety, personal safety (detection of fires, gas leak, etc), counterfeit (perfumes and wines) as well as biomedical applications.

Acknowledgements

Appendix A. Supplementary data

Supplementary material related to this article can be found, in the online version, at doi:https://doi.org/10.1016/j.snb.2019.127188.

References

[1] S. Öztürk, A. Kösemen, Z. Şen, N. Kılınç, M. Harbeck, Poly (3-methylthiophene) thin films deposited electrochemically on QCMs for the sensing of volatile organic compounds, Sensors 16 (2016) 423.

[2] S. Sankaran, S. Panigrahi, S. Mallik, Odorant binding protein based biomimetic sensors for detection of alcohols associated with Salmonella contamination in packaged beef, Biosens. Bioelectron. 26 (2011) 3103–3109.

[3] H.-H. Lu, Y.K. Rao, T.-Z. Wu, Y.-M. Tzeng, Direct characterization and quantification of volatile organic compounds by piezoelectric module chips sensor, Sens. Actuators B Chem. 137 (2009) 741–746.

[4] Q. Liu, H. Cai, Y. Xu, Y. Li, R. Li, P. Wang, Olfactory cell-based biosensor: a first step towards a neurochip of bioelectronic nose, Biosens. Bioelectron. 22 (2006) 318–322.

[5] T.-Z. Wu, Y.-R. Lo, E.-C. Chan, Exploring the recognized bio-mimicry materials for gas sensing, Biosens. Bioelectron. 16 (2001) 945–953.

[6] M. Mascini, M. Del Carlo, D. Compagnone, I. Cozzani, P.G. Tiscar, C. Mpamhanga, et al., Piezoelectric sensors based on biomimetic peptides for the detection of heat shock proteins (HSPs) in mussels, Anal. Lett. 39 (2006) 1627–1642.

[7] C. Baggiani, F. Biagioli, L. Anfossi, C. Giovannoli, C. Passini, G. Giraudi, Effect of the mimic structure on the molecular recognition properties of molecularly imprinted polymers for ochratoxin A prepared by a fragmental approach, React. Funct. Polym. 73 (2013) 833–837.

[8] M. Heurich, Z. Altintas, I. Tothill, Computational design of peptide ligands for ochratoxin A, Toxins 5 (2013) 1202–1218.

[9] M. Mascini, C. Montesano, M. Sergi, G. Perez, M. De Cicco, R. Curini, et al., Peptides trapping cocaine: docking simulation and experimental screening by solid phase extraction followed by liquid chromatography mass spectrometry in plasma samples, Anal. Chim. Acta 772 (2013) 40–46.

[10] M. Mascini, D. Pizzoni, G. Perez, E. Chiarappa, C. Di Natale, P. Pittia, et al., Tailoring gas sensor arrays via the design of short peptides sequences as binding elements, Biosens. Bioelectron. 93 (2017) 161–169.

[11] M. Del Carlo, G. Fusella, A. Pepe, M. Sergi, M. Di Martino, M. Mascini, et al., Novel oligopeptides based e-nose for food quality control: application to extra-virgin olive samples, Qual. Assur. Saf. Crop. Foods 6 (2014) 309–317.

[12] D. Compagnone, M. Faieta, D. Pizzoni, C. Di Natale, R. Paolesse, T. Van Caelenberg, et al., Quartz crystal microbalance gas sensor arrays for the quality control of chocolate, Sens. Actuators B Chem. 207 (2015) 1114–1120.

[13] D. Pizzoni, D. Compagnone, C. Di Natale, N. D'Alessandro, P. Pittia, Evaluation of aroma release of gummy candies added with strawberry flavours by gas-chromatography/mass-spectrometry and gas sensors arrays, J. Food Eng. 167 (2015) 77–86.

[14] M. Mascini, S. Gaggiotti, F. Della Pelle, C. Di Natale, S. Qakala, E. Iwuoha, et al., Peptide modified ZnO nanoparticles as gas sensors array for volatile organic compounds (VOCs), Front. Chem. 6 (2018) 105.

[15] S. Gaggiotti, M. Mascini, P. Pittia, F. Della Pelle, D. Compagnone, Headspace volatile evaluation of carrot samples—comparison of GC/MS and AuNPs-hpDNA-Based E-Nose, Foods 8 (2019) 293.

[16] S. Gaggiotti, B. Shkembi, G. Sacchetti, D. Compagnone, Study on volatile markers of pasta quality using GC-MS and a peptide based gas sensor array, LWT 114 (2019) 108364.

[17] N.T. Nguyet, V. Van Thu, T. Trung, P.H. Vuong, P.D. Tam, Highly sensitive DNA sensors based on cerium oxide nanorods, J. Phys. Chem. Solids 115 (2018) 18–25.

[18] P.A. Rasheed, N. Sandhyarani, Carbon nanostructures as immobilization platform for DNA: a review on current progress in electrochemical DNA sensors, Biosens. Bioelectron. 97 (2017) 226–237.

[19] A.C. Johnson, C. Staii, M. Chen, S. Khamis, R. Johnson, M. Klein, et al., DNA-decorated carbon nanotubes for chemical sensing, Semicond. Sci. Technol. 21 (2006) S17.

[20] N.J. Kybert, M.B. Lerner, J.S. Yodh, G. Preti, A.C. Johnson, Differentiation of complex vapor mixtures using versatile DNA–carbon nanotube chemical sensor arrays, ACS Nano 7 (2013) 2800–2807.

[21] N.J. Kybert, G.H. Han, M.B. Lerner, E.N. Dattoli, A. Esfandiar, A.C. Johnson, Scalable arrays of chemical vapor sensors based on DNA-decorated graphene, Nano Res. 7 (2014) 95–103.

[22] M. Mascini, S. Gaggiotti, F. Della Pelle, J. Wang, J.M. Pingarrón, D. Compagnone, Hairpin DNA-AuNPs as molecular binding elements for the detection of volatile organic compounds, Biosens. Bioelectron. 123 (2019) 124–130.

[23] Y. Hou, M. Genua, D. Tada Batista, R. Calemczuk, A. Buhot, P. Fornarelli, et al., Continuous evolution profiles for electronic-tongue-based analysis, Angew. Chemie Int. Ed. 51 (2012) 10394–10398.

[24] M. Genua, L.-A. Garçon, V. Mounier, H. Wehry, A. Buhot, M. Billon, et al., SPR imaging based electronic tongue via landscape images for complex mixture analysis, Talanta 130 (2014) 49–54.

[25] L.-A. Garçon, Y. Hou, M. Genua, A. Buhot, R. Calemczuk, D. Bonnaffé, et al., Landscapes of taste by a novel electronic tongue for the analysis of complex mixtures, Sens. Lett. 12 (2014) 1059–1064.

[26] L.-A. Garçon, M. Genua, Y. Hou, A. Buhot, R. Calemczuk, T. Livache, et al., A versatile electronic tongue based on surface plasmon resonance imaging and cross-reactive sensor arrays—a mini-review, Sensors 17 (2017) 1046.

[27] C. Hurot, S. Brenet, A. Buhot, E. Barou, C. Belloir, L. Briand, et al., Highly sensitive olfactory biosensors for the detection of volatile organic compounds by surface plasmon resonance imaging, Biosens. Bioelectron. 123 (2019) 230–236.

[28] S. Brenet, A. John-Herpin, F.-X. Gallat, B. Musnier, A. Buhot, C. Herrier, et al., Highly-selective optoelectronic nose based on surface plasmon resonance imaging for sensing volatile organic compounds, Anal. Chem. 90 (2018) 9879–9887.

[29] Y. Hou, M. Genua, L.-A. Garçon, A. Buhot, R. Calemczuk, D. Bonnaffé, et al., Electronic tongue generating continuous recognition patterns for protein analysis, JoVE (2014).

[30] K. Sasirekha, P. Baby, Agglomerative hierarchical clustering algorithm-a, Int. J. Sci. Res. Publ. 83 (2013) 83.

Sara Gaggiotti attempted both bachelor and master's degree in Food Science & Technology at the University of Teramo. Nowadays, she is a last-year Ph.D. student in Food Sciences at the University of Teramo, and she is the author of 4 in international journals. Her research field is focused on the development of rapid diagnostic tools for food quality and safety control.

Charlotte Hurot is an engineer graduated from Ecole Centrale de Lyon, France, in 2017. She is specialized in bioengineering and nanotechnology, and more specifically in the development of biosensors. She is currently pursuing her PhD thesis at the Commissariat à l'Energie Atomique et aux Energies Alternatives (CEA) in Grenoble (France), under the supervision of Dr. Yanxia Hou and Dr. Arnaud Buhot. Her PhD thesis focuses on improving the sensitivity and selectivity of optoelectronic noses.

Jonathan S. Weerakkody has his B.Sc., in Nanosystems Engineering from Louisiana Tech University, USA. Following which, with funding from the European commission, he completed a joint M.Sc in Nanoscience and Nanotechnology at KU Leuven (Belgium) and Université Grenoble-Alpes (France). He is currently pursuing his PhD, funded by the Nanoscience foundation, at the Commissariat à l'Energie Atomique et aux Energies Alternatives (CEA) in Grenoble (France). His main area of research is the development of electronic noses for VOC sensing in the gas phase based on Surface Plasmon Resonance imaging. In particular, he focuses on the study of the effect of temperature and humidity on VOC sensing using such a system.

Raphael Mathey is a biotechnology laboratory technician. He has worked in a multi-disciplinary environment at BioMerieux (joint team bMx/CEA-Leti) in France. Since 2013, he joined the laboratory SyMMES at the Commissariat à l'Energie Atomique et aux Energies Alternatives (CEA) in Grenoble (France). He has expertise in biochip development, molecular biology, bacteriology and surface functionalization. He participates in the development of biosensors for applications related to bacteriology as well as the development of the optoelectronic noses and tongues.

Arnaud Buhot is the head of the group Chemistry for the Recognition and Study of Biological Assemblies (CREAB) in the laboratory SyMMES at the Commissariat à l'Energie Atomique et aux Energies Alternatives (CEA) in Grenoble (France). His research activities aim at the conception, the development, the applications and the comprehension of biosensors mainly based on Surface Plasmon Resonance imaging detection and bio-molecular recognition (aptamers, peptides, etc). More particularly, he is working on optoelectronic noses and tongues.

Marcello Mascini is assistant professor in analytical chemistry. His research area was focused on the development of screening methods for fast and real time detection of analytes important for food, environmental and health analysis. The research interests were with a particular focus on new methods to develop bio-inspired and bio-mimetic systems in analytical application using molecular modeling and multivariate analysis.

Yanxia Hou obtained her PhD in Analytical Chemistry at Ecole Centrale de Lyon (France) in 2005. Since 2008, she has been employed by French National Center for Scientific Research (CNRS) as permanent scientific researcher. She has strong expertise on surface chemistry, surface functionalization and characterization, biosensors and biochips for the biomedical applications. Since 2008, she leads the development of novel optoelectronic noses and tongues based on SPRi in the laboratory of SyMMES, at the Commissariat à l'Energie Atomique et aux Energies Alternatives (CEA) in Grenoble (France). Her research interests include also nanotechnology such as the elaboration and engineering of hybrid multifunctional micro/nanoparticles for nanomedicine. She has published more than 30 scientific papers in peer-reviewed journals, 2 book chapters, and 4 patents. She is one of the co-founders and scientific counselor of the start-up company Aryballe Technologies, created in 2014 in Grenoble (France) for the miniaturization of the optoelectronic nose for digital olfaction.

Dario Compagnone has coordinated in the last 10 years the analytical chemistry group of the Faculty of Biosciences of the University of Teramo. He is author of over 170 papers on international scientific journals. His research interests are focussed on the development of sensing and biosensing strategies for the rapid detection of quality and safety markers of food.